

A global radiative-convective feedback

Laura D. Fowler and David A. Randall

Department of Atmospheric Science, Colorado State University, Fort Collins, Colorado

Abstract. We have investigated the sensitivity of the intensity of convective activity and atmospheric radiative cooling to radiatively thick upper-tropospheric clouds using a new version of the Colorado State University General Circulation Model. The model includes a bulk cloud microphysics scheme to predict the formation of cloud water, cloud ice, rain, and snow. The cloud optical properties are interactive and dependent upon the cloud water and cloud ice paths. We find that the formation of a persistent upper tropospheric cloud ice shield leads to decreased atmospheric radiative cooling and increased static stability. Convective activity is then strongly suppressed. In this way, upper-tropospheric clouds act as regulators of the global hydrologic cycle, and provide a negative feedback between atmospheric radiative cooling and convective activity.

Introduction

Stratiform anvil clouds significantly reduce the top-of-the-atmosphere outgoing longwave radiation, thus contributing strongly to the greenhouse effect of the atmosphere [Ackerman et al., 1988]. At solar wave lengths, bright anvils reflect solar radiation back to space [e.g., Ramanathan and Collins, 1991], while solar absorption by cirrus clouds strongly heats the upper troposphere [Ramaswamy and Ramanathan, 1989].

Studies with general circulation models have demonstrated that, by influencing the horizontal variations of the longwave cooling of the atmosphere, upper-tropospheric clouds also have a powerful influence upon the local intensity of convection and, in particular, the atmospheric circulation. Randall et al. [1989] and Slingo and Slingo [1988] showed that the horizontal variations of the atmospheric cloud longwave radiative forcing locally enhances large-scale rising motion, deep convective activity and cumulus precipitation in the region of strong longwave heating. This is a positive feedback that tends to increase the *local* intensity of convection. We call it a "radiative-dynamical-convective feedback." It is a local feedback because it depends on the horizontal variations of the longwave heating.

Here we report a *global* negative feedback loop involving the formation of upper-tropospheric stratiform clouds, atmospheric radiative cooling (ARC), and convective activity. We call it "a global radiative-convective feedback." It works as follows: Strong convective activity produces a radiatively thick upper-tropospheric cloud shield by detrainment of cloud water and cloud ice from the tops of cumulus towers. The formation of thick stratiform anvils and cirrus debris lead to a decreased ARC and a more statically stable atmosphere. Cumulus convection is then suppressed and the total precipitation rate decreases. The upper-level fractional cloudiness diminishes accordingly. The system equilibrates when the ARC and latent

heating are in balance, as shown in Fig. 1. The reduction in the precipitation rate due to decreased ARC does not necessarily occur in the same place where the ARC decreases; nevertheless, in a global average, the reduction in the ARC leads to a reduction in the latent heating. This is why we describe the feedback as "global." Figure 2 illustrates both the radiative-dynamical-convective feedback and the global radiative-convective feedback, and shows how they differ.

Model Description

We have investigated the impact of upper tropospheric stratiform clouds on the ARC and hydrologic cycle of the Colorado State University General Circulation Model (CSU GCM). A complete description of the CSU GCM may be found in Randall et al. [1989]. The model has recently been modified [Fowler and Randall, 1994; Fowler et al., 1994] to use a cloud microphysics scheme based on the bulk cloud microphysics equations described in Lin et al. [1983], and Rutledge and Hobbs [1983, 1984]. Five prognostic variables for the mass of water vapor, cloud water, cloud ice, rain, and snow are considered. Cloud water and cloud ice are predicted to form through large-scale condensation and deposition processes. An important additional source of cloud water and cloud ice is detrainment at the tops of cumulus towers. We assume that the fallspeeds of cloud water and cloud ice particles are negligible, although rain and snow precipitate, of course. The cumulus parameterization is a modified version of the Arakawa-Schubert parameterization [Arakawa and Schubert, 1974], as implemented by Lord et al. [1982]. The modifications include a prognostic cumulus kinetic energy [Randall and Pan, 1993], in place of strict quasi-equilibrium.

The parameterization of radiative transfer at infrared and solar wave lengths is described by Harshvardhan et al. [1987] and Harshvardhan et al. [1989]. At present, the cloud microphysics and radiation transfer parameterizations do not

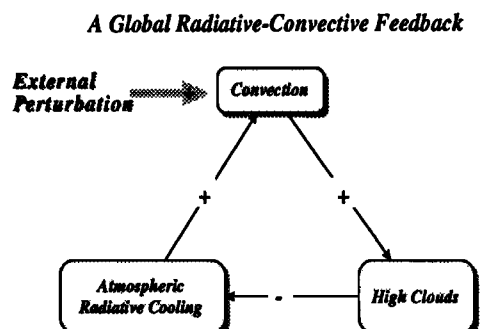


Figure 1. Schematic diagram illustrating the negative Global Radiative-Convective Feedback. An external perturbation tends to force more vigorous convection. This leads to more upper-tropospheric cloudiness, which reduces the atmospheric radiative cooling. Convection must then weaken to satisfy the global energy balance.

Copyright 1994 by the American Geophysical Union.

Paper number 94GL01711
0094-8534/94/94GL-01711\$03.00

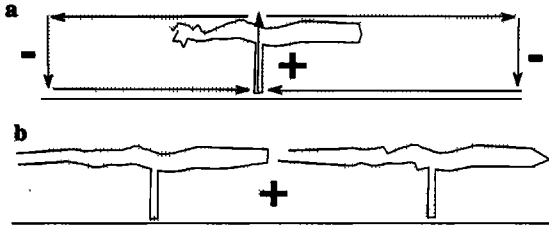


Figure 2. Illustration of the Radiative-Dynamical-Convective Feedback versus the Global-Radiative-Convective Feedback: (a) The Radiative-Dynamical-Convective Feedback, in which *horizontal gradients* in atmospheric radiative heating (indicated by + and -), associated with *horizontal gradients* in upper tropospheric cloudiness, favor rising motion and moisture convergence in the region of radiative warming, thus producing more upper tropospheric clouds locally, and so feeding back positively to increase the upper tropospheric cloudiness *locally*; (b) The Global Radiative-Convective Feedback, in which the *globally averaged* upper-tropospheric cloudiness induces a positive atmospheric longwave cloud radiative forcing (indicated by +) which reduces the *globally averaged* atmospheric radiative cooling, thus reducing the need for latent heat release, and so feeding back negatively to reduce the *globally averaged* upper tropospheric cloudiness.

use fractional cloudiness. No clouds are allowed to form above 100 mb. The parameterization of PBL clouds follows the formulation of Randall et al. [1985]. In the free troposphere, the fractional area of clouds is set equal to 1 if the cloud water or cloud ice paths is greater than 1 g m^{-2} . The formulation of the cloud radiative properties as a function of the cloud water and ice paths follows the formulation of Stephens [1978]. The cloud optical depth (τ) and cloud infrared emissivity (ϵ) are computed from

$$\tau = \frac{3}{2} \frac{W}{r_e} \quad \text{and} \quad \epsilon = 1 - \exp(-\kappa W) \quad (1)$$

where W is the cloud water or ice path (with dimensions of mass per unit area). The effective radius, r_e , is set equal to $10 \mu\text{m}$ and $30 \mu\text{m}$ for cloud water and cloud ice, respectively. The absorption coefficient, κ , is set equal to 0.13 and 0.08 g m^{-2} for cloud water and cloud ice, respectively. The single scattering albedo and the asymmetry factor are assumed to be the same for cloud water and cloud ice, and are equal to 0.99 and 0.85 , respectively. The radiative effects of rain and snow are neglected.

Experiment Design

Two 120-day simulations were performed, both corresponding to perpetual January conditions. Sea-surface temperatures were fixed in both runs. The control simulation (hereafter referred to as FRR) produces a simulated climate similar to that of the baseline simulation described in Fowler and Randall [1994] and Fowler et al. [1994]. In the experiment (hereafter referred to as SRH), an optically thick cloud envelope is produced by reducing the rates of autoconversion of cloud water (ice) to rain (snow) in the microphysics parameterization. The two runs were started with the same set of initial conditions. The only difference between them was the value of the prescribed threshold that controls the autoconversion of cloud water and cloud ice to rain and snow, respectively. In SRH, the threshold for autoconversion of cloud droplets to rain drops (q_{c0}) is set to 0.7 g kg^{-1} , and the threshold value for

autoconversion of cloud ice crystals to snow flakes (q_{i0}) is set to 1 g kg^{-1} . These values of q_{c0} and q_{i0} were used by Rutledge and Hobbs [1983] and Lin et al. [1983] to parameterize autoconversion processes in a mesoscale cloud model used to simulate warm and cold frontal bands. In FRR, the values of q_{c0} and q_{i0} are considerably smaller than in SRH, allowing for faster autoconversion of cloud water (ice) to rain (snow) and shorter lifetimes of clouds. We set q_{c0} equal to 0.1 g kg^{-1} and q_{i0} to 0.01 g kg^{-1} . Note that these are very large reductions relative to the values recommended by Rutledge and Hobbs [1983, 1984], and Lin et al. [1983]. As explained by Fowler et al. [1994], these values of q_{c0} and q_{i0} were chosen (tuned), in FRR, in order to obtain top-of-the-atmosphere radiation components in reasonable agreement with satellite observations. This tuning is needed because the present model does not have fractional cloudiness, and so does microphysics with grid-cell-averaged liquid and ice mixing ratios which are much smaller than their local counterparts would be in individual cloud elements.

Results

The various results are presented in terms of 30-day means computed from the last 30 days of the two simulations. The runs have reached an equilibrium state by day 90. The very strong sensitivity of the amount of suspended cloud ice (CI) to the threshold q_{i0} , is best seen in Fig. 3.a. The zonally averaged

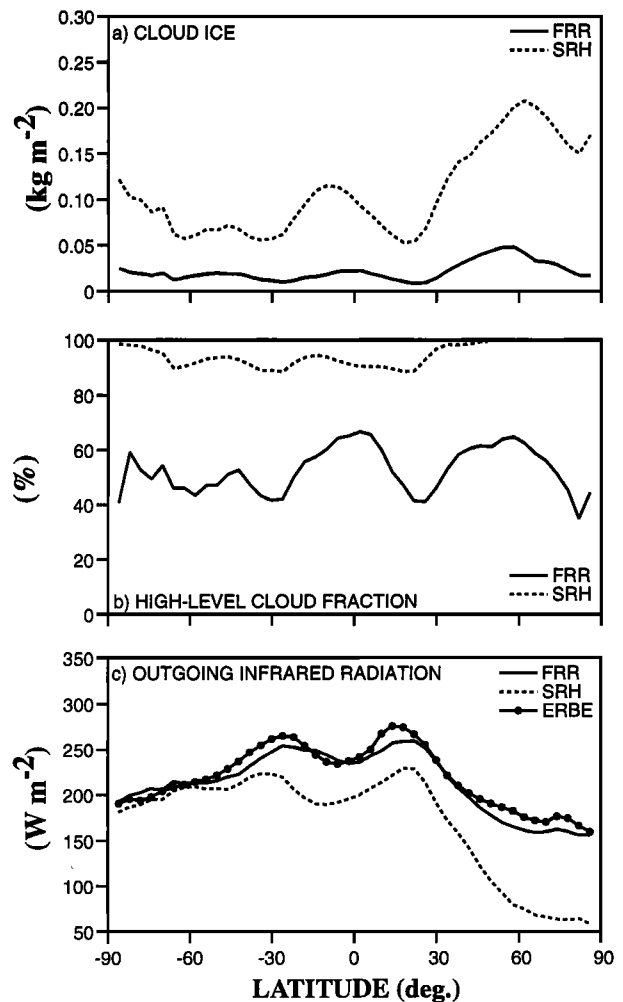


Figure 3. Zonally averaged distributions of the 30-day averaged (a) cloud ice mixing ratio, (b) high-level cloud fraction, (c) and outgoing infrared radiation simulated with FRR (solid line) and SRH (dotted line).

distribution of CI shows a primary maximum at high latitudes in the winter hemisphere in conjunction with cold temperatures, and a secondary maximum at low latitudes in conjunction with strong detrainment of cloud ice at the tops of cumulus towers. The simulated CI seems plausible but cannot be checked against satellite data at present, since no such data exist. These maxima and minima of CI are the strongest in the SRH run. The amount of suspended cloud water (CW) is shown to undergo a very similar increase as CI when q_{c0} varies from 0.1 to 0.7 g kg⁻¹. The increase in CW and CI from FRR to SRH, resulting from slower conversion of cloud water to rain and cloud ice to snow, is quite dramatic. Table 1 indicates that, on a global average, CW is increased by a factor of 4 while CI is increased by a factor of 5. As seen in Fig. 3.b, the increase in CW and CI between FRR and SRH produces a dramatic increase of upper-tropospheric cloudiness. The fractional coverage (in the monthly mean) of upper-tropospheric clouds drastically increases from a fairly realistic 54% in FRR to a very unrealistic 94% in SRH. The corresponding changes are 37% to 61% for middle-level clouds (between 700 mb and 400 mb), and 45% to 56% for low-level clouds (below 700 mb).

The effect of the formation of an optically thick cloud shield on the outgoing infrared radiation is also shown in Fig. 3.c, which compares the latitudinal distribution of the outgoing longwave radiation (OLR) obtained with FRR and SRH against ERBE (Earth Radiation Budget Experiment) satellite observations. The OLR from the ERBE data is an ensemble average for the four January months spanning 1985 to 1988. There is fairly good agreement in the OLR between FRR and the ERBE data. FRR is able to correctly reproduce the minimum OLR observed at low latitudes but slightly underestimates stronger outgoing longwave radiation in the subtropics. For solar radiation, FRR slightly underestimates α between 30°N and 30°S, and fails to correctly reproduce the increase in α with latitude. The changes in OLR and α between FRR and SRH are also very dramatic. The 40% increase in the upper-tropospheric cloud fraction yields a 40 W m⁻² decrease in OLR and 13% increase in α , as shown in Table 1. The decrease in OLR from FRR to SRH becomes huge north of 30°N in the winter hemisphere.

The increase in the static stability of the atmosphere between FRR and SRH can be inferred from Fig. 4. In response to the decreased ARC, cumulus precipitation is almost completely suppressed in SRH. The globally-averaged cumulus precipitation rate drops from 1.23 mm day⁻¹ in FRR to 0.04 mm day⁻¹ in SRH. The globally-averaged large-scale precipitation rate remains about the same between the two experiments (1.99

Table 1: Globally averaged values of the components of the hydrologic cycle and planetary radiation budget obtained in the FRR and SRH simulations.

Global averages	FRR	SRH
Cloud water (kg m ⁻²)	0.06	0.25
Cloud ice (kg m ⁻²)	0.02	0.10
Cumulus precipitation (mm day ⁻¹)	1.23	0.04
Large-scale precipitation (mm day ⁻¹)	1.99	1.86
Total precipitation (mm day ⁻¹)	3.22	1.90
Outgoing longwave radiation (W m ⁻²)	225	185
Planetary albedo (%)	28	41
Atmospheric radiative cooling (W m ⁻²)	73	33

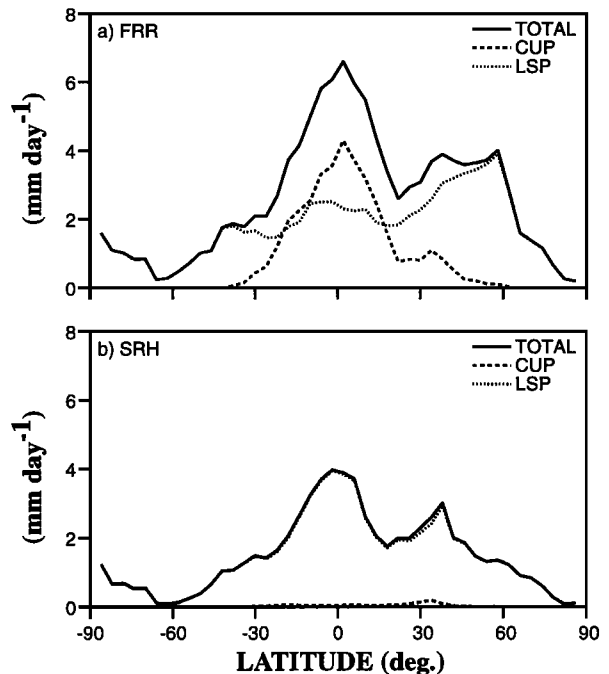


Figure 4. Zonally averaged distributions of the 30-day averaged cumulus, large-scale, and total precipitation rates simulated with (a) FRR, and (b) SRH.

mm day⁻¹ in FRR versus 1.86 mm day⁻¹ in SRH). Figure 4 shows that the large-scale precipitation rate increases in the tropics by about 2 mm day⁻¹ while it also decreases by the same amount at about 50°N. Table 1 shows that the globally averaged total precipitation rate is reduced by about 41% in SRH. This is a direct response to the reduced ARC between SRH and FRR (40 W m⁻²).

Finally, Fig. 5 shows the impact of the reduced atmospheric radiation cooling and convective activity on the latitudinal and vertical distributions of temperature. The presence of an upper-tropospheric cloud shield yields a warming of the whole troposphere which remains small at low levels, due our use of fixed sea-surface temperatures, and is very large at high altitudes. Figure 5 shows that the zonally averaged temperature increases by as much as 30 K at the tropopause height in the summer hemisphere.

Discussion

We have illustrated a global radiative-convective feedback through the use of an extreme scenario (case SRH), which was realized by producing a persistent, radiatively thick, upper-tropospheric cloud ice shield with the cloud microphysics scheme. The effects of the upper-tropospheric clouds are to reduce the ARC by about 56%, and to increase the static stability of the atmosphere. Convective activity is almost completely suppressed by the strong increase in static stability. The total precipitation rate is decreased by about 40%. Large-scale precipitation increases, and this is made possible by an overall increase in the relative humidity and the precipitable water.

On a global scale, and assuming that sea-surface temperatures remain fixed, the interaction between the ARC and latent heat release may be summarized as follows. The globally-averaged energy balance of the atmosphere approximately satisfies

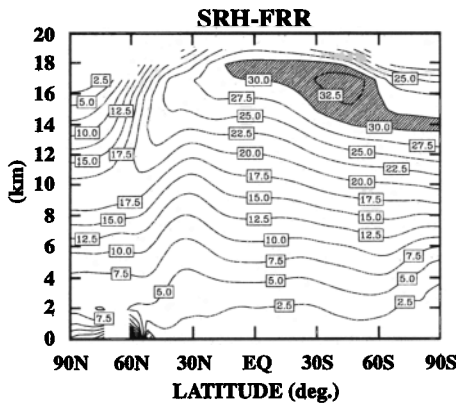


Figure 5. Latitude-height cross sections of the 30-day averaged temperature difference between SRH and FRR. Heavy shading corresponds values greater than 30 K.

$$L_c P \equiv LW_{\text{atmclr}} - SW_{\text{atmclr}} - LWCRF_{\text{toa}} \quad (2)$$

Here, $LW_{\text{atmclr}} - SW_{\text{atmclr}}$ is the net clear-sky radiative cooling of the atmosphere, and $LWCRF_{\text{toa}}$ is the longwave cloud radiative forcing at the top of the atmosphere.

We assume that the latent heating is approximately proportional to the cloud longwave radiative forcing so that $LWCRF_{\text{toa}} = \alpha L_c P$, where α is a constant. This is reasonable because both $LWCRF_{\text{toa}}$ and P are primarily associated with deep clouds. Then, $L_c P$ satisfies

$$L_c P \equiv \frac{LW_{\text{atmclr}} - SW_{\text{atmclr}}}{1 + \alpha} \quad (3)$$

This shows that larger values of α tend to decrease the precipitation rate. In the real atmosphere, $LWCRF_{\text{toa}}$ and $L_c P$ are approximately equal to 30 W m^{-2} and 90 W m^{-2} , respectively, so that $\alpha \approx 1/3$.

Although strongly exaggerated, our numerical results illustrate one important way that the longwave cloud forcing associated with upper-tropospheric stratiform clouds produced by deep convection can strongly affect the climate.

Radiatively thick upper-tropospheric clouds produce, on a global scale, a strongly negative feedback, by reducing the intensity of latent heat release through decreased atmospheric radiative cooling. This negative "global radiative-convective" cloud feedback is at work in a climate system that also contains other cloud feedbacks, both positive and negative. The combined effects of these several cloud feedbacks on the climate system can only be determined after much further study.

Acknowledgments. This research was sponsored by the National Science Foundation under grant ATM-8907414, by NASA under grant NAG-1653, and by the ARM program of the U. S. Department of Energy under grant DE-FG02-92ER61363, all to Colorado State University. Prof. S. Rutledge of Colorado State University provided valuable guidance in the development of the cloud microphysics parameterization and the interpretation of the results. Prof. G.L. Stephens made helpful comments on the manuscript.

References

- Ackerman, T.P., K.-N. Liou, F.P.J. Valero, and L. Pfister, Heating rates in tropical anvils, *J. Atmos. Sci.*, **45**, 1606-1623, 1988.
- Arakawa, A., and W.H. Schubert, The interaction of a cumulus cloud ensemble with the large-scale environment. Part I, *J. Atmos. Sci.*, **31**, 674-701, 1974.
- Fowler, L.D., D.A. Randall, and S.A. Rutledge, Liquid and ice cloud microphysics in the CSU general circulation model: Part I. Model description and simulated microphysical processes, 1994 (Submitted to *J. Climate*).
- Fowler, L.D., D.A. Randall, Liquid and ice cloud microphysics in the CSU general circulation model. Part II: Impact on cloudiness, the Earth's radiation budget, and the general circulation of the atmosphere, 1994 (Submitted to *J. Climate*).
- Harshvardhan, R. Davies, D.A. Randall, and T.G. Corsetti, A fast radiation parameterization for atmospheric circulation models, *J. Geophys. Res.*, **92**, 1009-1016, 1987.
- Harshvardhan, D.A. Randall, T.G. Corsetti, and D.A. Dazlich, Earth radiation budget and cloudiness simulations with a general circulation model, *J. Atmos. Sci.*, **46**, 1922-1942, 1989.
- Lin, Y.-L., R.D. Farley, and H.D. Orville, Bulk parameterization of the snow field in a cloud model, *J. Atmos. Sci.*, **22**, 1065-1092, 1983.
- Lord, S.J., W.C. Chao, and A. Arakawa, Interaction of a cumulus cloud ensemble with the large-scale environment, Part IV: The discrete model, *J. Atmos. Sci.*, **39**, 104-113, 1982.
- Ramanathan, V., The role of Earth Radiation Budget studies in climate and general circulation research, *J. Geophys. Res.*, **92**, 4075-4094, 1987.
- Ramanathan, V., and W. Collins, Thermodynamic regulation of ocean warming by cirrus clouds deduced from observations of the 1987 El Niño, *Nature*, **351**, 27-32, 1991.
- Ramaswamy, V., and V. Ramanathan, Solar absorption by cirrus clouds and the maintenance of the tropical upper troposphere thermal structure, *J. Atmos. Sci.*, **46**, 2293-2310, 1989.
- Randall, D.A., J.A. Abeles, and T.G. Corsetti, Seasonal simulations of the planetary boundary layer and boundary-layer stratocumulus clouds with a general circulation model, *J. Atmos. Sci.*, **42**, 641-676, 1985.
- Randall, D.A., Harshvardhan, D.A. Dazlich, and T.G. Corsetti, Interactions among radiation, convection, and large-scale dynamics in a general circulation model, *J. Atmos. Sci.*, **46**, 1943-1970, 1989.
- Randall, D.A., and D.-M. Pan, 1993: Implementation of the Arakawa-Schubert cumulus parameterization with a prognostic closure. In *Cumulus Parameterization*, a Meteorological Monograph published by the American Meteorological Society, K. Emanuel and D. Raymond, Eds., pp. 137 - 144.
- Rutledge, S.A., and P.V. Hobbs, The mesoscale and microscale structure and organization of cloud bands and precipitation in middle latitude cyclones. VIII: A model for the "Seeder Feeder" process in warm frontal bands, *J. Atmos. Sci.*, **40**, 1185-1206, 1983.
- Rutledge, S.A., and P.V. Hobbs, The mesoscale and microscale structure of clouds and precipitation in midlatitude cyclones. XII: A diagnostic modelling study of precipitation development in narrow cold-frontal rainbands, *J. Atmos. Sci.*, **41**, 2949-2972, 1984.
- Slingo, A., and J.M. Slingo, The response of a general circulation model to cloud longwave radiative forcing. I: Introduction and initial experiments, *Q. J. R. Meteorol. Soc.*, **114**, 1027-1062, 1988.
- Stephens, G.L., Radiation profiles in extended water clouds, II: Parameterization schemes, *J. Atmos. Sci.*, **35**, 2123-2132, 1978.

L.D. Fowler and D.A. Randall, Department of Atmospheric Science, Colorado State University, Fort Collins, CO 80523. (e-mail: laura@silkrack.atmos.colostate.edu)

(Received April 6, 1994; revised June 2, 1994; accepted June 21, 1994)